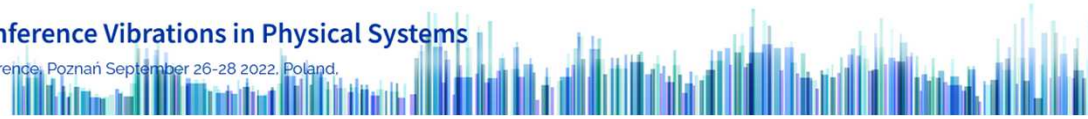




30th Conference Vibrations in Physical Systems

Vibsyst Conference, Poznań September 26-28 2022, Poland.



## THE EXPERIMENTAL STAND FOR OBSERVATION AND CONTROL OF DYNAMICS OF AN EXTENDED ATWOOD'S MACHINE

**Paweł OLEJNIK\*, Krzysztof PEPA, Godiya YAKUBU, Jan AWREJCWICZ**

*Department of Automation, Biomechanics and Mechatronics, Lodz University of Technology  
1/15 Stefanowski Str., 90-537 Lodz, Poland*

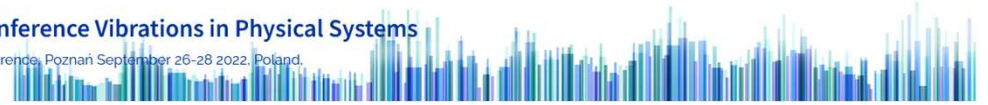
*\*presenter (pawel.olejnik@p.lodz.pl)*

*Monday 15:30 PM, 26.09.2022  
Lecture Center of Poznan University of Technology*



30th Conference Vibrations in Physical Systems

Vibsys Conference, Poznań September 26-28 2022, Poland.



# SCOPE OF THE PRESENTATION

Pawel OLEJNIK\*, Krzysztof PEPA, Godiya YAKUBU, Jan AWREJCWICZ  
*Department of Automation, Biomechanics and Mechatronics, Lodz University of Technology*

- Presentation of the physical model
- Mathematical description of a system with friction
- Basic numerical modeling of the dynamical behavior
- Realization of the experimental stand
- Summary



# THE SWINGING ATWOOD'S MACHINE

Paweł OLEJNIK\*, Krzysztof PEPA, Godiya YAKUBU, Jan AWREJCWICZ  
*Department of Automation, Biomechanics and Mechatronics, Lodz University of Technology*



30th Conference Vibrations in Physical Systems

Vibsys Conference, Poznań September 26-28 2022, Poland.

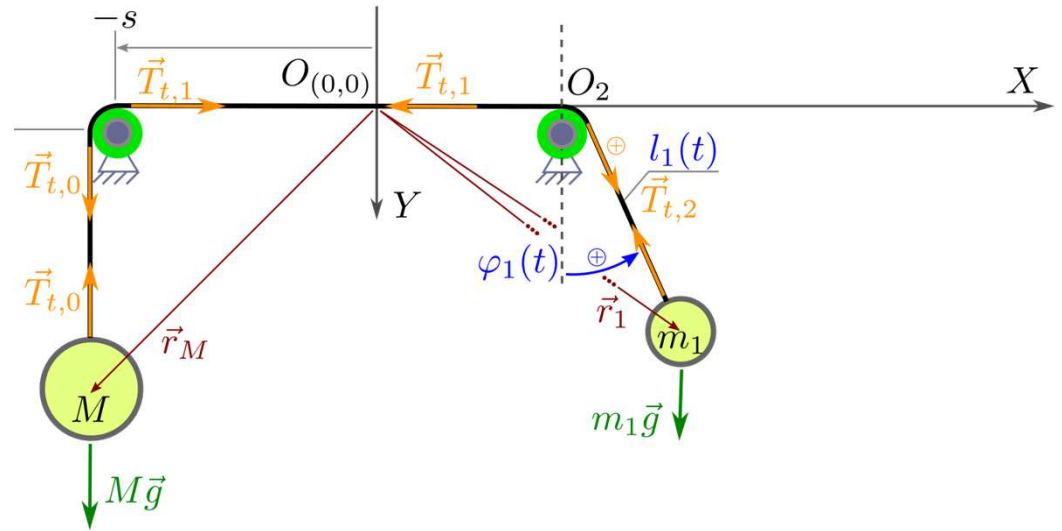
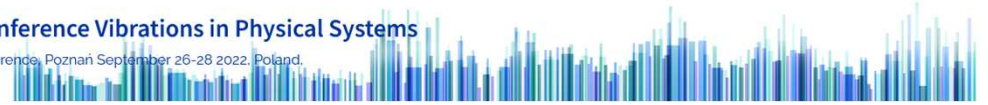


Figure 1.a.



# THE MODIFIED SWINGING ATWOOD'S MACHINE

Paweł OLEJNIK\*, Krzysztof PEPA, Godiya YAKUBU, Jan AWREJCWICZ  
*Department of Automation, Biomechanics and Mechatronics, Lodz University of Technology*



30th Conference Vibrations in Physical Systems

Vibsys Conference, Poznań September 26-28 2022, Poland.

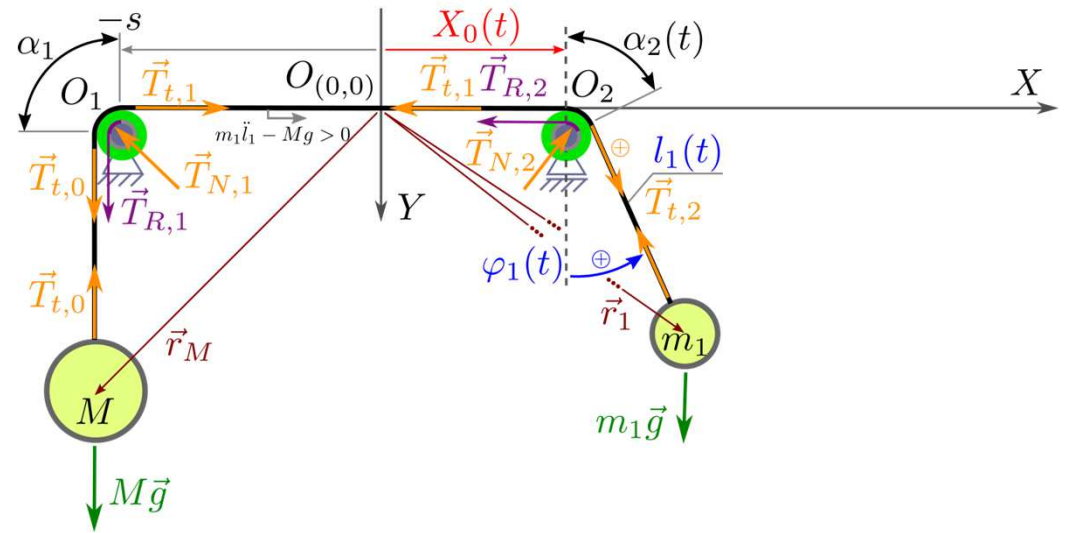
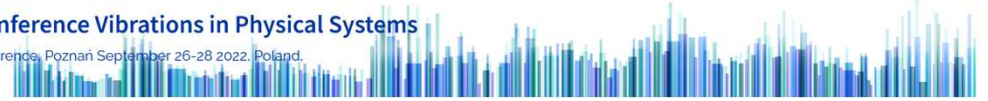


Figure 1.b.



# THE MODIFIED SWINGING ATWOOD'S MACHINE

Paweł OLEJNIK\*, Krzysztof PEPA, Godiya YAKUBU, Jan AWREJCWICZ  
 Department of Automation, Biomechanics and Mechatronics, Lodz University of Technology



30th Conference Vibrations in Physical Systems

Vibsys Conference, Poznań September 26-28 2022, Poland.

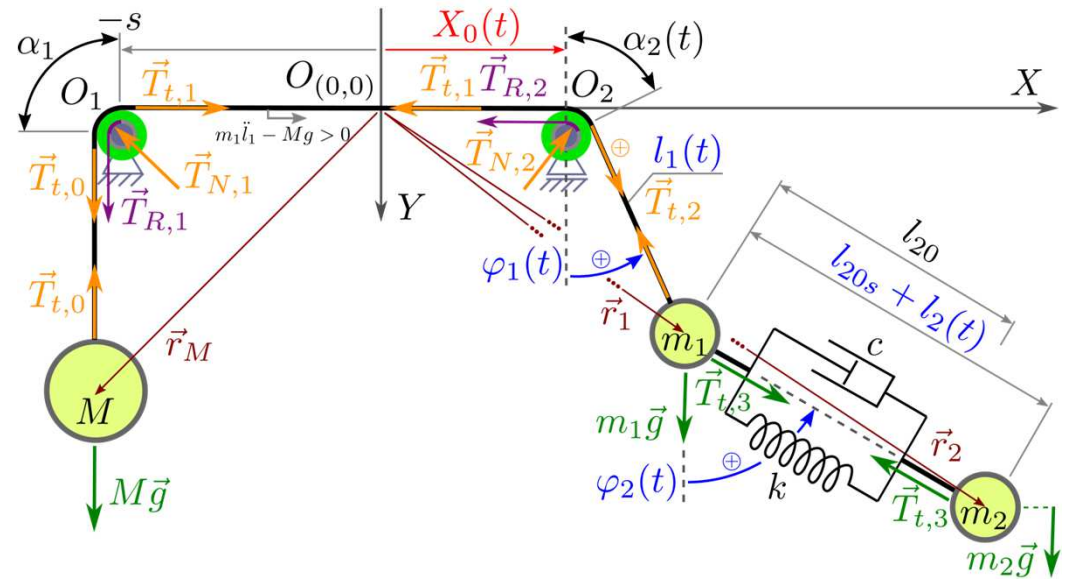
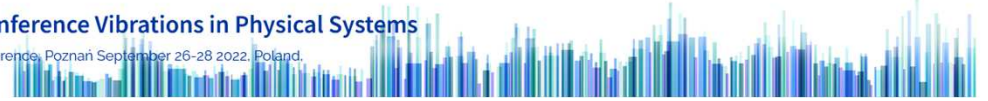


Figure 1.c.

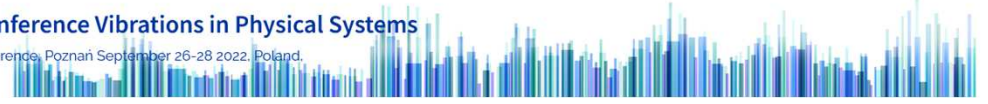


## MATHEMATICAL DESCRIPTION

Using Newton's second law of dynamics to establish the extended SAM equations of motion, we assumed that the links are massless and the masses are focused in points that connect subsequent cords. We consider air drag forces acting on the counterweight mass  $M$  and the mass of the first pendulum  $m_1$ . However, due to complexity, we neglect the drag force acting on  $m_2$ . The vector to the counter mass  $M$  in the assumed system of coordinates is introduced:

$$\vec{r}_M = [X_M, Y_M], \quad \text{for} \quad X_M = -s, \quad Y_M = L_n - l_1(t) - s - X_0(t), \quad (1)$$

where  $X_0(t) = f_0 \sin(\omega t)$  – time function of periodic kinematic excitation, which is measured from the origin of the global coordinate system  $O_{(0,0)}$  to the right in  $X$  direction;  $s$  – distance in the  $X$  direction from  $O_{(0,0)}$  to the fixed support point  $O_1$ ;  $L_n$  – length of the entire cord between the centers of the counterweight mass  $M$  and the pendulum  $m_1$ .



## MATHEMATICAL DESCRIPTION

The sum of forces acting on mass  $M$  in  $Y$ -direction only follows:

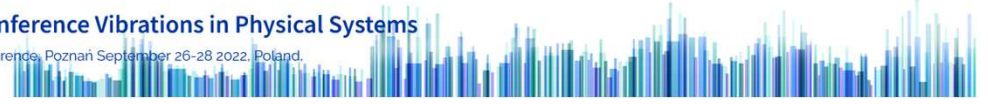
$$\begin{aligned} M\vec{r}_M &= \sum \vec{F}_M \\ &= [0, -T_{t,0} + Mg], \end{aligned} \quad (2)$$

where the  $T_R$  represents the total friction force in both pulley bearings, including Coulomb and viscous friction.

Defining the length  $L_2(t) = l_{20s} + l_2(t)$  of the second pendulum, we can introduce the vectors of both pendulous bodies with the coordinates of vectors  $\vec{r}_i$ :

$$\begin{aligned} \vec{r}_1 &= [X_1, Y_1] = [X_0(t) + l_1(t)\sin\varphi_1(t), l_1(t)\cos\varphi_1(t)], \\ \vec{r}_2 &= [X_2, Y_2] = [X_1 + L_2(t)\sin\varphi_2(t), Y_1 + L_2(t)\cos\varphi_2(t)] \end{aligned} \quad (3)$$

at  $l_{20s} = l_{20} + l_{2st}$ ,  $l_{20}$  – free length of the spring stiffness  $k$ ,  $l_{2st} = m_2g/k$  – static elongation of the spring.



## MATHEMATICAL DESCRIPTION

Now we define the forces acting on the first and second pendulum's masses  $m_1$  and  $m_2$ , respectively:

$$\begin{aligned}\vec{F}_1 &= [F_{1X}, F_{1Y}] = [-(T_{t,2} + T_R) \sin \varphi_1(t) + T_{t,3} \sin \varphi_2(t), -(T_{t,2} + T_R) \cos \varphi_1(t) + T_{t,3} \cos \varphi_2(t) + m_1 g], \\ \vec{F}_2 &= [F_{2X}, F_{2Y}] = [-T_{t,3} \sin \varphi_2(t), -T_{t,3} \cos \varphi_2(t) + m_2 g],\end{aligned}\quad (4)$$

including an expression of force in the spring-damper Maxwell coupling-based model:

$$T_{t,3} = kl_2(t) + c\dot{l}_2(t).\quad (5)$$

The equations of motion are given in the general form:

$$\begin{aligned}m_i \ddot{r}_{iX}(t) &= F_{iX}, \\ m_i \ddot{r}_{iY}(t) &= F_{iY}, \quad \text{for } i = 1, 2,\end{aligned}\quad (6)$$

where  $F_{iX}$ ,  $F_{iY}$  – force components acting at mass  $m_i$ , in the  $(X, Y)$ -plane. The Newton model 6 state the equations of dynamic balance of forces acting in the system.



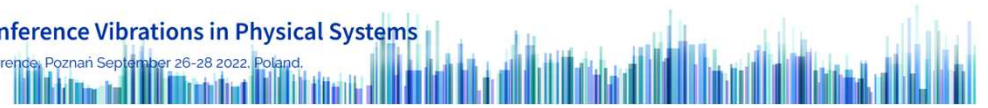


## MATHEMATICAL DESCRIPTION

The system of four second-order ordinary differential equations of motion governs the system's dynamical behavior (the general coordinates:  $l_1(t)$ ,  $l_2(t)$ ,  $\varphi_1(t)$ ,  $\varphi_2(t)$ ):

$$\begin{aligned}\ddot{l}_1 &= \frac{1}{m_1 + M} \left( T_{t,3} \cos \varphi_{21} - \ddot{X}_0 (m_1 \sin \varphi_1 + M) + m_1 (g \cos \varphi_1 + l_1 \dot{\varphi}_1^2) - T_R - Mg \right), \\ \ddot{l}_2 &= \frac{1}{2m_1 m_2 (m_1 + M)} \left( M m_2 T_{t,3} (\cos 2\varphi_{21} - 1) + m_1 m_2 \left( M \ddot{X}_0 (2 \cos \varphi_{21} + \sin(\varphi_2 - 2\varphi_1) - \sin \varphi_2) \right. \right. \\ &\quad \left. \left. + gM (2 \cos \varphi_{21} + \cos(\varphi_2 - 2\varphi_1) + \cos \varphi_2) + 2((M l_1 \dot{\varphi}_1 + T_R) \cos \varphi_{21} + (m_1 + M) L_2 \dot{\varphi}_2^2 - T_{t,3}) \right) \right. \\ &\quad \left. - 2m_1 T_{t,3} (m_1 + M) \right) \\ \ddot{\varphi}_1 &= \frac{1}{m_1 l_1} \left( T_{t,3} \sin \varphi_{21} - m_1 (g \sin \varphi_1 + \ddot{X}_0 \cos \varphi_1 + 2l_1 \dot{\varphi}_1) \right), \\ \ddot{\varphi}_2 &= \frac{1}{2m_1 L_2 (m_1 + M)} \left( -M T_{t,3} \sin 2\varphi_{21} - M m_1 \left( g (2 \sin \varphi_{21} + \sin(\varphi_2 - 2\varphi_1) + \sin \varphi_2) \right. \right. \\ &\quad \left. \left. + \ddot{X}_0 (2 \sin \varphi_{21} - \cos(\varphi_2 - 2\varphi_1) + \cos \varphi_2) + 2l_1 \dot{\varphi}_1^2 \sin \varphi_{21} \right) - 2m_1 (T_R \sin \varphi_{21} + 2(m_1 + M) l_2 \dot{\varphi}_2) \right).\end{aligned}\tag{7}$$

where  $\varphi_{21} = \varphi_2 - \varphi_1$ ,  $\ddot{X}_0 = -\omega^2 f_0 \sin \omega t$ ,  $f_0$  is maximum amplitude of the kinematic excitation.



## MATHEMATICAL DESCRIPTION (FRICTION)

Now a model of the friction force in the pulley bearings arranged horizontally in a row will be presented; as shown in the Fig. 1. We consider Coulomb and viscous friction. In the first assumption, the rotation of the pulleys is caused by friction resulting from the stresses in the cord. It should be noted that the diameter of the pulley is disregarded, but must not be too small, due to the difficult to describe change of the tension force when bending the cord.

The Coulomb friction model is used to model tangential forces between the contact surface, which depends on the relative speed of the two dry solid surfaces in contact [Olejnik *et al.*, 2018]. Models of Coulomb friction have been widely used, and various compensation techniques exist. However, we start with the simple model as a guide to introduce the Coulomb and viscous friction model.

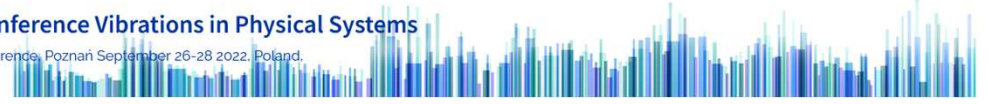


## MATHEMATICAL DESCRIPTION (FRICTION)

After deriving the equations of the dynamics of the motion of the triple pendulum (reduced to a double) suspended by means of an inextensible cord through two pulleys, the friction occurring on the surface of the rotational contact of the rotational sliding bearing as well as on the contact surface of the cord and the rotating sleeve of this bearing was omitted. Bringing our dynamic model closer to the real system, we introduce the bearing resistance  $T_{R,i}$  in the form of both Coulomb and viscous friction, while assuming that the cord rolls along the outer surface of the pulleys placed on bearing sleeve without slippage. From the mathematical point of view, we had  $T_{t,i} = T_{t,i-1}$ , so the tension forces were equal before and after a pulley. However, after taking into account both effects of the resistance in the rotation of the bearings, i.e., Coulomb friction force  $T_{c,i}$  and the force of viscous friction  $T_{v,i}$  at  $i$ -th pulley in the points  $O_i$ , we have:

$$T_{t,i} = T_{t,i-1} + T_{R,i} = T_{t,i-1} + T_{c,i} + T_{v,i}, \quad \text{for } i = 1, 2. \quad (8)$$

The above formula describes a force equilibrium for a cord guided around a pulley under the consideration of a friction force  $T_{R,i}$  at the cord velocity  $\dot{l}_1$ .



## MATHEMATICAL DESCRIPTION (FRICTION)

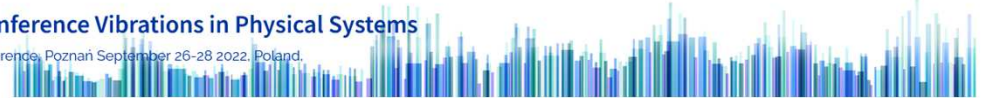
Viscous friction depends on the speed of movement of the cord (and the associated pulley sliding bearing) and a certain coefficient. Assuming that the cord is constantly tensioned at whole length  $L_n$ , which is true for the considered mechanical system, the speed of cord movement about each pulley will be the first derivative of the change in the length  $l_1$  of the pendulum of the mass  $m_1$ . In this case, it is sufficient to assume a certain constant value of the viscous friction coefficient denoted by  $d_i$  for each of the pulleys, so we arrive at the formula  $T_{v,i} = d_i \dot{l}_1$ . The first component of the drag seems to be more difficult, namely Coulomb friction. In this case, we need to determine the normal force exerted by the pulling forces on both sides of the pulleys, which operate at angles that depend on the wrap angle  $\alpha_i$  for a particular pulley. It should be noted that  $\alpha_2$  changes in time due to the dynamic change in the angle of the mass pendulum  $m_1$ . The wrapping angles for the first (fixed) and the second pulley moving horizontally with the amplitude  $X_0(t)$  are as follows:  $\alpha_1 = \pi/2$ ,  $\alpha_2 = \pi/2 - \varphi_1$ , respectively.

The Coulomb friction force in  $i$ -th pulley bearing follows from the basic definition:

$$T_{c,i} = \text{sgn}(\dot{l}_1) \mu_i T_{N,i}. \quad (9)$$

Following [Kraus *et al.*, 2015],  $T_{N,i}$  is the  $i$ -th force of normal reaction of a particular pulley bearing:

$$T_{N,i} = \sqrt{T_{t,i}^2 - 2T_{t,i}T_{t,i-1} \cos \alpha_i + T_{t,i-1}^2}. \quad (10)$$



## MATHEMATICAL DESCRIPTION (FRICTION)

The normal force in Eq. (10) acts at the bisection of the wrapping angle of contact of the cord with a pulley. This allows for the following approximation:

$$T_{N,i} \approx \frac{T_{t,i} + T_{t,i-1}}{2} \sqrt{2(1 - \cos \alpha_i)}. \quad (11)$$

The relationship for the tension forces acting between the successive pulleys is unknown. For this purpose, we eliminate  $T_{N,i}$  by substituting Eq. (11) in (9) and then  $T_{c,i}$  in (8). Solving the resulting algebraic equation with respect to  $T_{t,i}$ , we get:

$$T_{t,i} = \frac{T_{t,i-1} \tilde{T}_{c,i} + 2(T_{v,i} + T_{t,i-1})}{\tilde{T}_{c,i} - 2} \quad (12)$$

for  $\tilde{T}_{c,i} = \text{sgn}(\dot{l}_1) \mu_i \sqrt{2(1 - \cos \alpha_i)}$  and  $T_{v,i} = d_i \dot{l}_1$ , for  $i = 1, 2$ .

The additional term reflecting the total frictional resistance  $T_R$ , being an external force to the mechanical system and existing in both pulley bearings  $O_i$  can be found as a sum of differences  $T_{R,i} = T_{t,i} - T_{t,i-1}$ ; see Eq. (8), i.e.:  $T_R = T_{R,1} + T_{R,2}$ , where initially, the first tension force  $T_{t,0} = Mg - m_1 \ddot{l}_1$ ; see Fig. 1.



# THE MODIFIED SWINGING ATWOOD'S MACHINE

Paweł OLEJNIK\*, Krzysztof PEPA, Godiya YAKUBU, Jan AWREJCWICZ  
 Department of Automation, Biomechanics and Mechatronics, Lodz University of Technology



30th Conference Vibrations in Physical Systems

Vibsys Conference, Poznań September 26-28 2022, Poland.

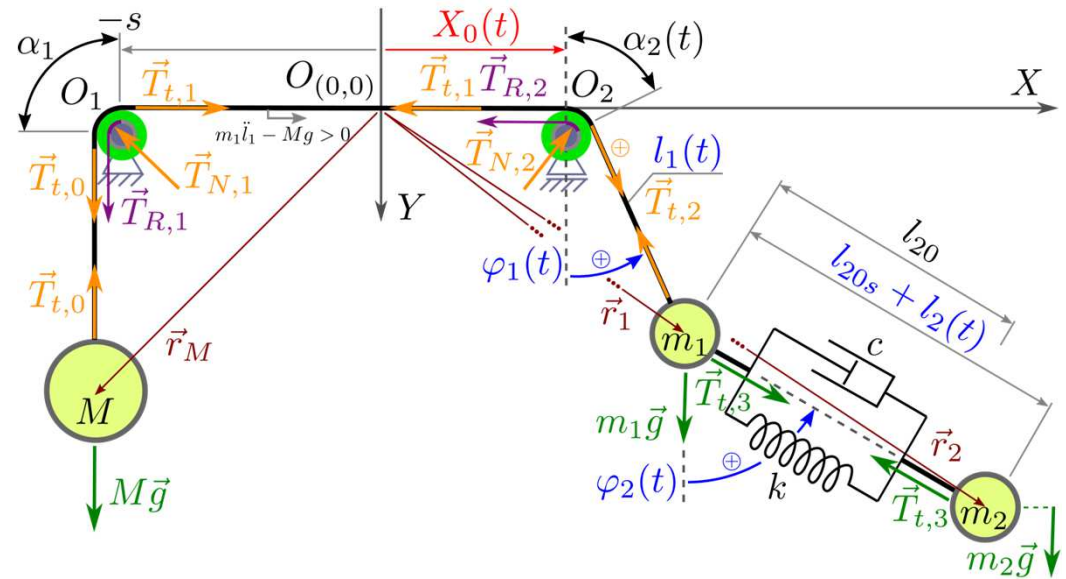
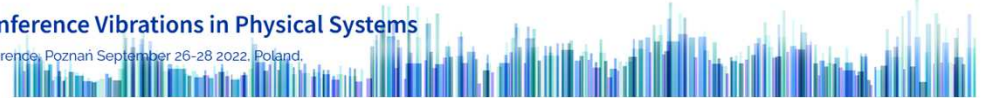
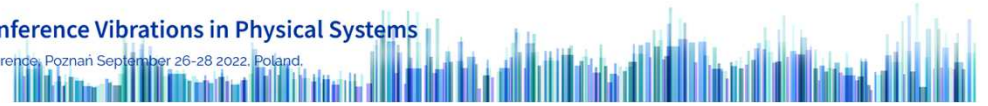
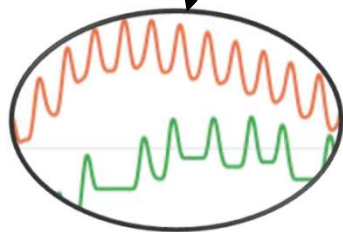
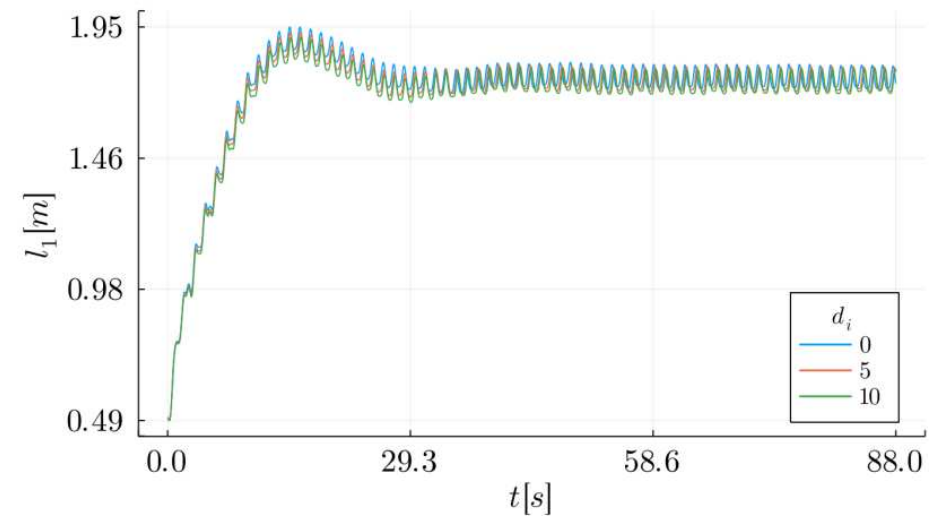
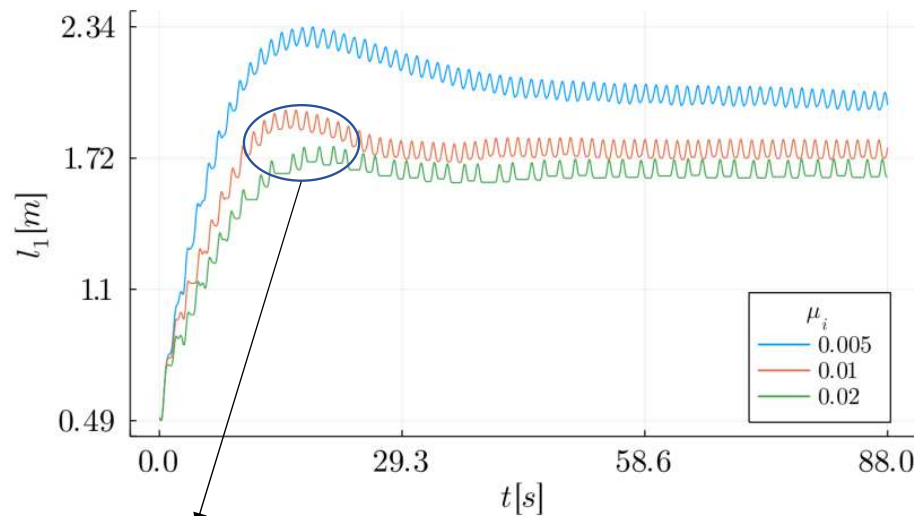


Figure 1.c.



# BASIC NUMERICAL MODELING

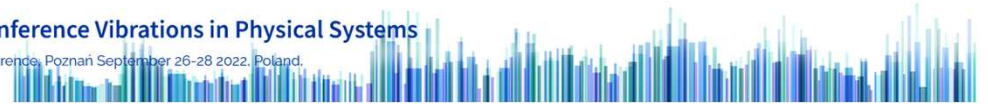
Influence of variation of the static friction coefficient  $\mu_i$  at  $d_i = 0$  (a), and the viscous friction coefficient  $d_i$  at  $\mu_i = 0.01$  (b) on the transient dynamical response of the first pendulum body.



(a)

(b)

Figure 2.



# REALIZATION OF THE EXPERIMENTAL STAND



Photo 1.





# REALIZATION OF THE EXPERIMENTAL STAND



Photo 2.



# REALIZATION OF THE EXPERIMENTAL STAND

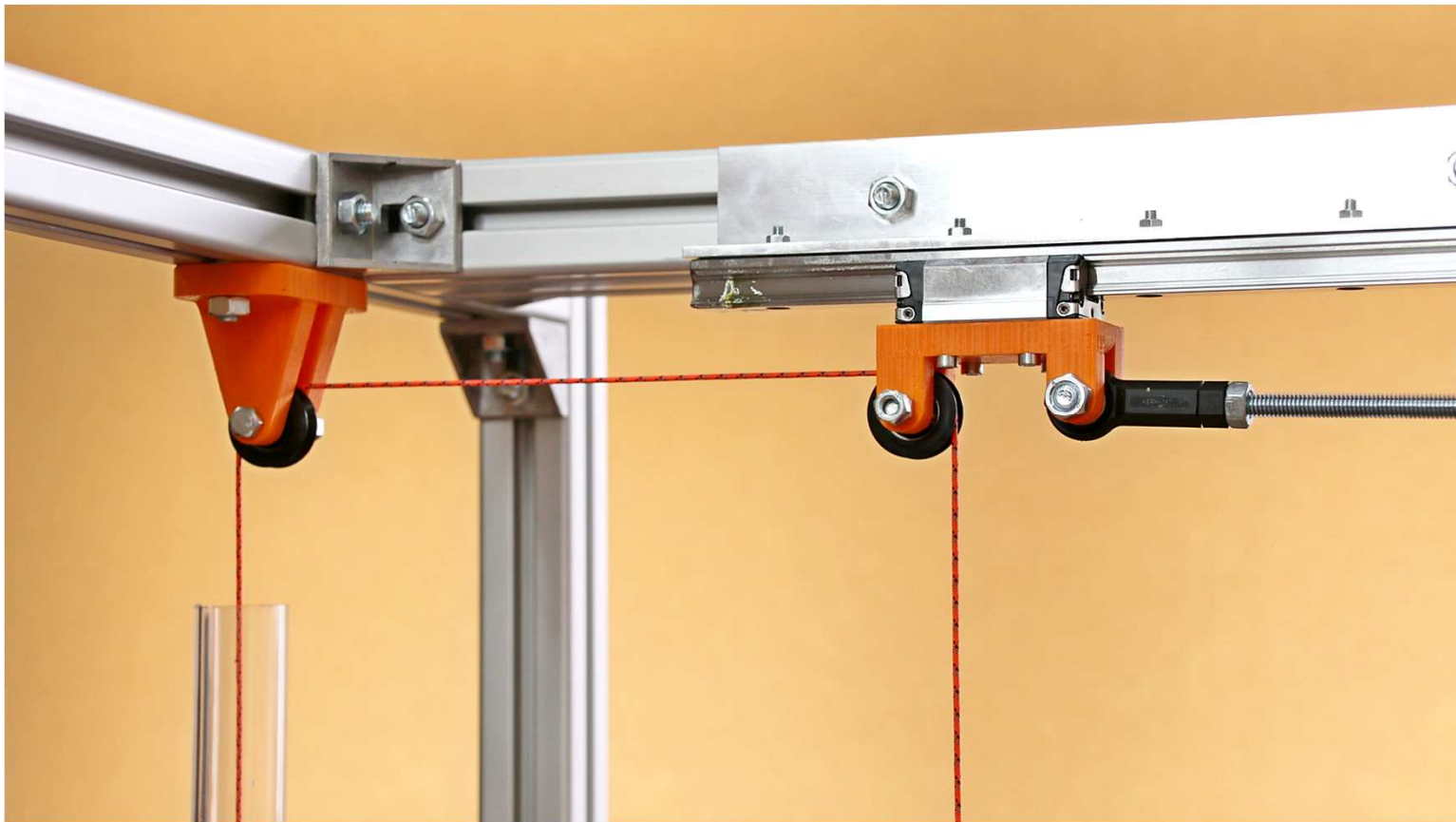


Photo 3.



# REALIZATION OF THE EXPERIMENTAL STAND

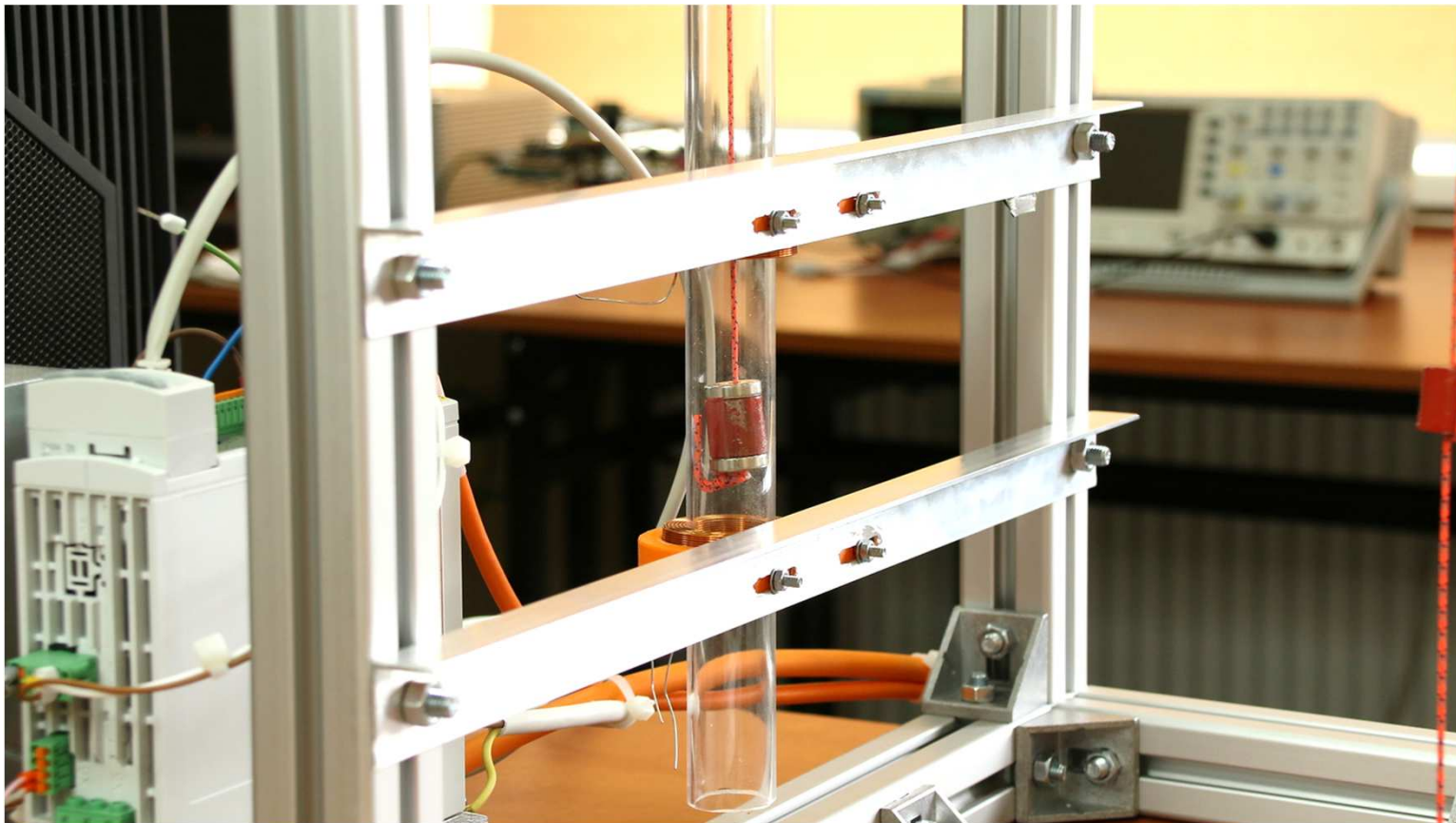


Photo 4.



# REALIZATION OF THE EXPERIMENTAL STAND

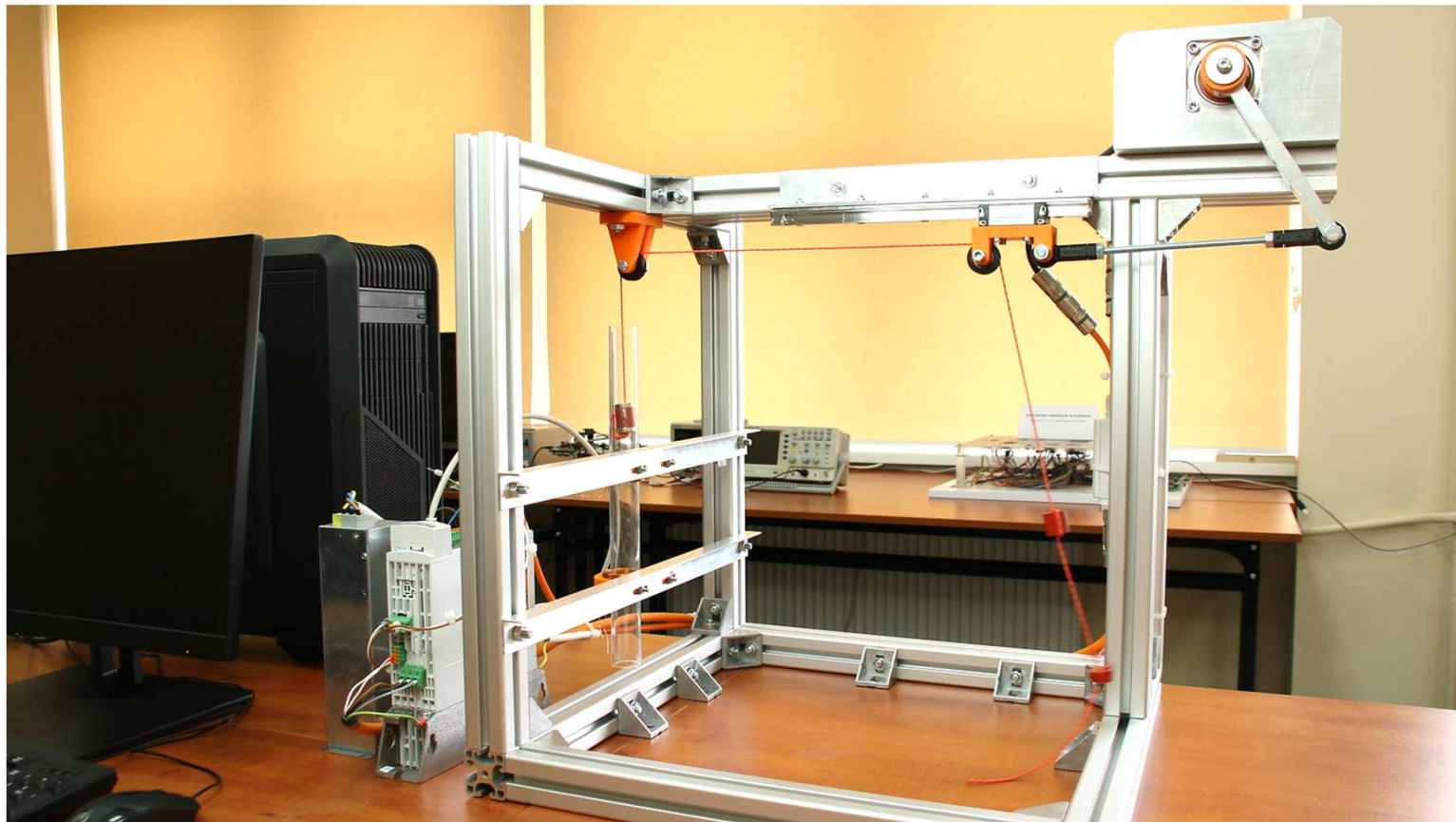
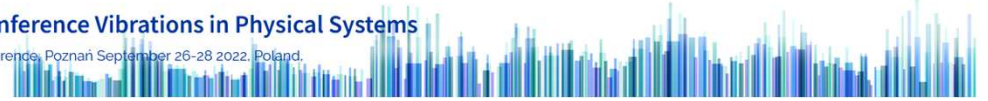


Photo 5.



## SUMMARY

- Observations of an unprecedented multi-mass system for testing and analysis of complex load (e.g., cranes) vibrations were initiated.
- A mathematical description of the friction system has been developed.
- Basic numerical modeling of the dynamic behavior of the 4-DoF system confirms the correctness of the adopted mathematical description. After the first numerical tests, the ability of the system to mostly maintain the quasi-periodic behavior is found.
- The experimental stand is under construction, but first trials confirm the difficulty of maintaining a stable dynamic response.
- It is intended to use a counter mass barrier consisting of two discontinuously forced electromagnets to control the test mass.

**ACKNOWLEDGEMENT:** This research was funded by Narodowe Centrum Nauki grant number 2019/35/B/ST8/00980 (NCN Poland).



30th Conference Vibrations in Physical Systems

Vibsyst Conference, Poznań September 26-28 2022, Poland.

**Thank you for your attention**

**Paweł OLEJNIK\*, Krzysztof PEPA, Godiya YAKUBU, Jan AWREJCWICZ**

*Department of Automation, Biomechanics and Mechatronics, Lodz University of Technology  
1/15 Stefanowski Str., 90-537 Lodz, Poland*

*\*presenter (pawel.olejnik@p.lodz.pl)*

*Monday 15:30 PM, 26.09.2022  
Lecture Center of Poznan University of Technology*